# Chains of Condensed $RuSm_{6/2}$ Octahedra in $Sm_3RuMg_7$ – A Ternary Ordered Version of the $Ti_6Sn_5$ Type

Stefan Linsinger and Rainer Pöttgen

Institut für Anorganische und Analytische Chemie, Universität Münster,
Corrensstraße 30, 48149 Münster, Germany

Reprint requests to R. Pöttgen. E-mail: pottgen@uni-muenster.de

*Z. Naturforsch.* **2011**, *66b,* 565 – 569; received March 31, 2011

The magnesium-rich intermetallic compound $Sm_3RuMg_7$ was synthesized by induction melting of the elements. Single crystals were grown by slow cooling of the polycrystalline sample. The structure was characterized by powder and single-crystal X-ray diffraction: ordered $Ti_6Sn_5$ type, $P6_3/mmc$, $Z$ = 2, $a$ = 1034.1(2), $c$ = 611.3(1) pm, $wR2$ = 0.0216, 399 $F^2$ values and 19 parameters. The ruthenium atoms have slightly distorted octahedral samarium coordination. These $RuSm_{6/2}$ octahedra (Ru–Sm 279 pm) are condensed *via* common faces leading to chains in the $c$ direction which are arranged in the form of a hexagonal rod packing. Between these rods the Mg2 atoms build chains of face-sharing trigonal prisms. Alternately these prisms are centered by Mg3 or capped by Mg1 atoms on the rectangular faces. Within the magnesium substructure the Mg–Mg distances range from 303 to 335 pm. The Mg3 site shows slight mixing with samarium, leading to the composition $Sm_{3.16}RuMg_{6.84}$ for the investigated crystal. The compounds $RE_3RuMg_7$ ($RE$ = Gd, Tb) are isotypic.

*Key words:* Magnesium, Rare Earth Compounds, Crystal Structure

## Introduction

Recent structural and magnetochemical investigations of various intermetallic compounds of the type $Ce_xRu_yX_z$ ($X$ = Mg, Cd, Zn, Al, In, Sn) have revealed a quite unique behavior. The compounds $Ce_3Ru_2In_3$ [1], $Ce_{16}Ru_8In_{37}$ [2], $Ce_2Ru_2In_3$ [3], $Ce_3Ru_2In_2$ [3], $CeRu_{0.88}In_2$ [4], CeRuSn [5 – 7], $Ce_2RuZn_4$ [8, 9], CeRuAl [10 – 12], $CeRu_2Mg_5$ [13], and $Ce_{23}Ru_7X_4$ ($X$ = Mg, Cd) [14, 15] show short Ce–Ru distances down to 230 pm, directly associated with intermediate or mixed cerium valence. For those compounds where the Ce–Ru distances are extremely short, the observed structure type is singular, and no isotypic compounds with the neighboring rare earth elements are observed.

If the shortening of the Ce–Ru distances is not that pronounced, or if a complex structure contains multiple, crystallographically independent cerium sites, a given cerium compound $Ce_xRu_yX_z$ shows just a reduced cell volume within a series of rare earth compounds. This is the case for $Ce_{23}Ru_7X_4$ ($X$ = Mg, Cd) [14, 15]. In the structurally closely related series of $RE_4$RuMg compounds [16] the $Ce_4$RuMg volume smoothly fits into the Iandelli plot, indicating trivalent cerium.

We have recently started a more systematic phase analytical investigation of the neighboring $RE$-Ru-$X$ systems. While we observed isotypic compounds in the series $RE_{23}Ru_7X_4$ ($X$ = Mg, Cd) [14, 15] and $RE_4$RuMg [16], PrRuSn (TiNiSi type) [17] and CeRuSn (CeCoAl superstructure) [5] adopt completely different structure types, driven by the valency of the rare earth element. The $RE$-Ru-Mg systems are even more complex. With cerium we found the intermediate-valence compounds $CeRu_2Mg_5$ [13] and $Ce_2Ru_4Mg_{17}$ [18] which crystallize both with their own structure types, again with short Ce–Ru distances. Parallel experiments with the heavier rare earth elements led to a new series of $RE_3RuMg_7$ ($RE$ = Sm, Gd, Tb) compounds with ordered $Ti_6Sn_5$ [19] type structure. The preparation and structure determination of these phases are reported herein.

## Experimental Section

### Synthesis

Starting materials for the preparation of the $RE_3RuMg_7$ ($RE$ = Sm, Gd, Tb) samples were ingots of the rare earth elements (Johnson Matthey), ruthenium powder (Allgemeine Gold- und Silberscheideanstalt, Pforzheim) and a magnesium rod (Alfa Aesar; the surface layer of the rod was re-

0932–0776 / 11 / 0600–0565 $ 06.00

moved on a turning lathe), all with stated purities better than 99.9 %. The rare earth metal ingots were cut into smaller pieces and arc-melted [20] into small buttons under an argon atmosphere. The argon was purified with molecular sieves, silica gel and titanium sponge (900 K). The rare earth buttons, ruthenium powder and pieces of the magnesium rod (3 : 1 : 7 atomic ratio) were sealed in tantalum tubes under an argon pressure of *ca.* 700 mbar. These ampoules were then sealed in silica tubes for oxidation protection, placed in a resistance furnace (Nabertherm, model: HTC 08/16), heated to about 1473 K and kept at that temperature for 8 h. Then the temperature was lowered to 673 K within 96 h, and the samples were annealed at this temperature for another 96 h. The products could easily be separated from the crucible. No reactions with the container material were observed. The $RE_3$RuMg$_7$ samples are stable in air over weeks. Single crystals exhibit metallic luster while ground powders are grey.

### *EDX data*

The bulk samples and the selected single crystal were studied by energy-dispersive analyses of X-rays (EDX) using a Zeiss EVO MA10 scanning electron microscope with $RE$F$_3$, ruthenium and MgO as standards. The experimentally observed compositions were close to the ideal one, and no impurity elements were observed.

### *X-Ray diffraction*

The polycrystalline $RE_3$RuMg$_7$ samples were characterized by Guinier powder patterns (Cu$K_{\alpha1}$ radiation, $\alpha$-quartz: $a$ = 491.30, $c$ = 540.46 pm as internal standard). The Guinier camera was equipped with an imaging plate (Fuji-film, BAS-1800 readout system). The hexagonal lattice parameters (Table 1) were obtained from least-squares fits of the powder data. Correct indexing was ensured by intensity calculations [21].

An irregularly shaped single crystal was selected from the Sm$_3$RuMg$_7$ sample by mechanical fragmentation and investigated by Laue photographs on a Buerger camera in order to check the quality for an intensity data collection. A data set was collected at r. t. using a STOE IPDS-II image plate system (graphite-monochromatized Mo$K_\alpha$ radiation; $\lambda$ = 71.073 pm) in oscillation mode. A numerical absorption correction was applied to this data set. All relevant crystallographic data are listed in Table 2.

Table 1. Lattice parameters (Guinier powder and single-crystal data) of the ternary magnesium compounds $RE_3$RuMg$_7$.

| Compound | $a$ (pm) | $c$ (pm) | $V$ (nm$^3$) |
|---|---|---|---|
| Sm$_3$RuMg$_7$ | 1034.8(2) | 613.00(9) | 0.5684 |
| Sm$_{3.16(1)}$RuMg$_{6.84(1)}$[a] | 1034.1(2) | 611.3(1) | 0.5661 |
| Gd$_3$RuMg$_7$ | 1026.4(2) | 610.22(6) | 0.5568 |
| Tb$_3$RuMg$_7$ | 1022.3(3) | 607.4(2) | 0.5497 |

[a] Single crystal data.

Table 2. Crystal data and structure refinement for Sm$_{3.16(1)}$RuMg$_{6.84(1)}$, space group $P6_3/mmc$, $Z$ = 2.

| | |
|---|---|
| Empirical formula | Sm$_{3.16(1)}$RuMg$_{6.84(1)}$ |
| Formula weight, g mol$^{-1}$ | 741.2 |
| Unit cell dimensions | Table 1 |
| Calculated density, g cm$^{-3}$ | 4.35 |
| Crystal size, $\mu$m$^3$ | 20 × 20 × 50 |
| Transm. ratio (max/min) | 1.22 |
| Absorption coefficient, mm$^{-1}$ | 17.7 |
| $F$(000), e | 644 |
| $\theta$ range for data collection, deg | 2 – 32 |
| Range in $hkl$ | ±15, ±15, ±8 |
| Total no. reflections | 5572 |
| Independent reflections / $R_\text{int}$ | 399 / 0.0695 |
| Reflections with $I \geq 2\sigma(I)$ / $R_\sigma$ | 315 / 0.0466 |
| Data / parameters | 399 / 19 |
| Goodness-of-fit on $F^2$ | 0.844 |
| $R1$ / $wR2$ for $I \geq 2\sigma(I)$ | 0.0260 / 0.0200 |
| $R1$ / $wR2$ for all data | 0.0463 / 0.0216 |
| Extinction coefficient | 0.00087(11) |
| Largest diff. peak / hole, e Å$^{-3}$ | 0.80 / −1.55 |

Table 3. Atomic coordinates and isotropic displacement parameters (pm$^2$) for Sm$_{3.16(1)}$RuMg$_{6.84(1)}$. $U_\text{eq}$ is defined as one third of the trace of the orthogonalized $U_\text{ij}$ tensor. $M$ is occupied by 84.3(4) % Mg and 15.7(4) % Sm.

| Atom | W. position | $x$ | $y$ | $z$ | $U_\text{eq}$ |
|---|---|---|---|---|---|
| Sm | 6$h$ | 0.13049(2) | 2$x$ | 1/4 | 119(1) |
| Ru | 2$a$ | 0 | 0 | 0 | 111(2) |
| Mg1 | 6$h$ | 0.77352(13) | 2$x$ | 1/4 | 175(6) |
| Mg2 | 6$g$ | 1/2 | 0 | 0 | 161(5) |
| $M$ | 2$c$ | 1/3 | 2/3 | 1/4 | 172(9) |

Table 4. Anisotropic displacement parameters (pm$^2$) for Sm$_{3.16(1)}$RuMg$_{6.84(1)}$. The anisotropic displacement factor exponent takes the form: $-2\pi^2[(ha^*)2U_{11}+\ldots+2hka^*b^*U_{12}]$.

| Atom | $U_{11}$ | $U_{22}$ | $U_{33}$ | $U_{23}$ | $U_{13}$ | $U_{12}$ |
|---|---|---|---|---|---|---|
| Sm | 124(1) | 117(2) | 113(2) | 0 | 0 | 58(1) |
| Ru | 119(3) | $U_{11}$ | 95(6) | 0 | 0 | 60(1) |
| Mg1 | 139(8) | 212(12) | 197(16) | 0 | 0 | 106(6) |
| Mg2 | 168(8) | 167(10) | 149(14) | −35(10) | −18(5) | 84(5) |
| $M$ | 154(10) | $U_{11}$ | 209(17) | 0 | 0 | 77(5) |

### *Structure refinement*

Careful examination of the data set showed a hexagonal lattice with high Laue symmetry and systematic extinctions 0 0 $l$ only observed for $l$ = 2$n$. This led to the space groups $P6_3/mmc$, $P6_3mc$, and $P6_322$, of which the space group with the highest symmetry, $P6_3/mmc$, was found to be correct. The starting atomic parameters were deduced by Direct Methods with SHELXS-97 [22], and the structure was refined using SHELXL-97 [23] (full-matrix least-squares on $F^2$) with anisotropic atomic displacement parameters for all sites. The

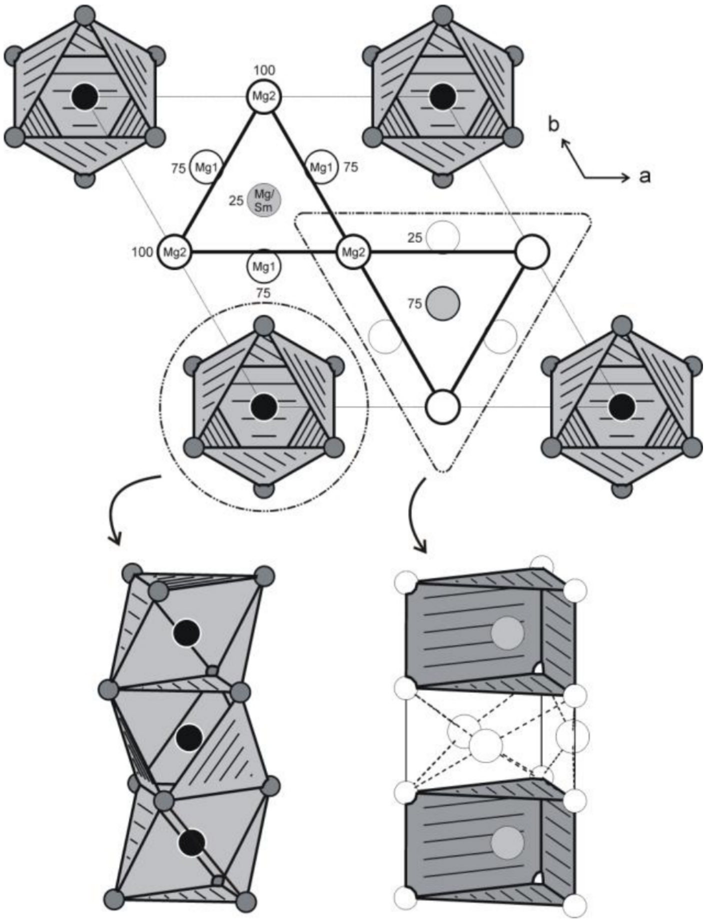

Fig. 1. (top) Projection of the $Sm_{3.16}RuMg_{6.84}$ structure onto the *xy* plane. Samarium, ruthenium, and magnesium atoms are drawn as light grey, black filled, and black open circles, respectively. Atom designations and heights are given in one part of the drawing. The octahedral and trigonal prismatic building groups are emphasized. (bottom) Cutouts of the chains of condensed octahedra and trigonal prisms extending along the *c* axis.

2*c* site was initially refined with the scattering power of a magnesium atom, however, the resulting displacement parameter was too small, indicating significantly higher scattering power on this position. Keeping the interatomic distances for this site and the results of $Sm_{3.92}Ru_{1.16}Mg_{0.92}$ [16] in mind, this site was refined with a mixed Mg/Sm occupancy leading to the composition $Sm_{3.16}RuMg_{6.84}$ for the investigated crystal. The final difference Fourier synthesis revealed no significant residual peaks (Table 2). The atomic parameters and interatomic distances are listed in Tables 3 and 4.

Further details of the crystal structure investigation may be obtained from Fachinformationszentrum Karlsruhe, 76344 Eggenstein-Leopoldshafen, Germany (fax: +49-7247-808-666; e-mail: crysdata@fiz-karlsruhe.de, http://www.fiz-informationsdienste.de/en/DB/icsd/depot_anforderung.html) on quoting the deposition number CSD-422864.

## Discussion

Besides the already discovered intermetallic compounds $RE_4RuMg$ ($RE$ = La-Nd, Sm, Gd-Ho) [16], $RE_{23}Ru_7Mg_4$ ($RE$ = La, Ce, Pr, Nd) [14], $CeRu_2Mg_5$ [13], and $Ce_2Ru_4Mg_{17}$ [18], our phase analytical studies in the *RE*-Ru-Mg systems now revealed the isotypic phases $RE_3RuMg_7$ ($RE$ = Sm, Gd, Tb). The existence of this new structure type is limited to these three rare earth elements. Attempts with the lighter (Pr, Nd) and heavier (Dy, Ho) rare earth elements resulted in ternary compounds with different composition and different structure. The lattice parameters (Table 5) of the $RE_3RuMg_7$ compounds decrease from the samarium to the terbium compound as expected from the lanthanoid contraction.

Inspection of the Pearson code hP22 and the Wyckoff sequence 194, $h^2gca$ in the Pearson Crystal Data Base [24] readily reveals isotypism with $Ti_6Sn_5$ [19]. This structure type has so far been observed for only few binary compounds and some ternary variants with mixed occupancies [25 – 30]. The magnesium compounds $RE_3RuMg_7$ are a new ternary ordered ver-

Table 5. Interatomic distances (pm) in $Sm_{3.16(1)}RuMg_{6.84(1)}$ calculated with the single-crystal lattice parameters. Standard deviations are all equal or smaller than 0.4 pm. All distances within the first coordination spheres are listed.

| | | | | | |
|---|---|---|---|---|---|
| Sm: 2 | Ru | 279.3 | Mg1: 4 | Mg2 | 303.3 |
| 2 | Mg1 | 350.7 | 2 | Mg1 | 331.5 |
| 2 | Mg1 | 352.7 | 2 | Sm | 350.7 |
| 1 | *M* | 363.3 | 2 | Sm | 352.7 |
| 4 | Mg2 | 368.8 | 2 | *M* | 360.6 |
| 4 | Sm | 384.8 | Mg2: 4 | Mg1 | 303.3 |
| 2 | Sm | 404.8 | 2 | Mg2 | 305.7 |
| Ru: 6 | Sm | 279.3 | 2 | *M* | 335.4 |
| 2 | Ru | 305.7 | 4 | Sm1 | 368.8 |
| | | | *M*: 6 | Mg2 | 335.4 |
| | | | 6 | Mg1 | 360.6 |
| | | | 3 | Sm | 363.3 |

sion of this atomic arrangement, *i. e.* Sm (Ti1) on 6*h*, Ru (Sn2) on 2*a*, Mg1 (Sn1) on 6*h*, Mg2 (Ti2) on 6*g*, and Mg/Sm (Sn3) on 2*c*. In view of these differing substitutions, and thus a changing bonding pattern, the relation between $Ti_6Sn_5$ and $Sm_3RuMg_7$ should be called isopointal [31, 32] rather than isotypic.

A projection of the $Sm_3RuMg_7$ structure onto the *xy* plane is presented in Fig. 1. The structure consists of two main structural building units. The samarium atoms form an octahedral coordination around the ruthenium atoms. The Ru–Sm distances of 279 pm are even smaller than the sum of the covalent radii [33] of 290 pm and we can therefore assume substantial Sm–Ru bonding. Similar short Sm–Ru distances occur in $Sm_3Ru$ ($Fe_3C$ type, 281 – 291 pm) and $Sm_5Ru_2$ ($Mn_5C_2$ type, 275 – 302 pm) [34]. Adjacent ruthenium atoms between the $Sm_6Ru$ octahedra are at Ru–Ru distances of 306 pm, half the *c* parameter. They are distinctly longer than the average Ru–Ru distance of 268 pm in *hcp* ruthenium [35]. The $Sm_6Ru$ octahedra are condensed *via* common triangular faces forming chains along the *c* axis (Fig. 1), arranged in the form of a hexagonal rod packing. This is a new structural motif in the family of $RE_xT_yMg_z$ intermetallics [36]. So far, only three-dimensional networks of condensed $RE_6Ru$ trigonal prisms have been observed in the $RE_4RuMg$ series [16].

The second characteristic building unit concerns the magnesium substructure. The Mg2 atoms at $z = 0$, 1/2, and 1 build up a Kagomé network with Mg2–Mg2 distances of 306 pm within the triangles. These distances are even slightly smaller than the average Mg–Mg distance of 320 pm in *hcp* magnesium [35]. Stacking of these Kagomé networks leads to trigonal prismatic voids with centers at $z$ = 1/4 and 3/4 on the threefold axis. As emphasized at the lower right-hand part of Fig. 1, every other prism is filled with a magnesium atom, a rather unusal coordination. This site has six Mg2 neighbors at 335 pm and six further Mg1 neighbors at the much longer distance of 361 pm. The rectangular faces of these filled trigonal prisms are capped by three samarium atoms from the chains of condensed octahedra at *M*–Sm of 363 pm. The trigonal prismatic site shows mixed occupancy. As observed for many of the $RE_4T$Mg phases [36, and refs. therein], and especially for $Sm_{3.92}Ru_{1.16}Mg_{0.92}$ [16], we observe a small percentage of samarium on this position. The *M*-Mg2 distance of 335 pm is in agreement with both the sum of the covalent radii for Sm+Ru and the distances in *hcp* Mg.

The empty trigonal prisms are capped by Mg1 on the rectangular faces with a Mg1–Mg2 distance of 303 pm. These are the shortest Mg–Mg distances in the $Sm_{3.16}RuMg_{6.84}$ structure. Such Mg–Mg distances typically occur in ternary magnesium-rich compounds, *e. g.* $CeRu_2Mg_5$ [13] or $TbCuMg_4$ [37].

### *Acknowledgements*

We thank Dipl.-Ing. U. C. Rodewald for the intensity data collection. This work was financially supported by the Deutsche Forschungsgemeinschaft.

[1] Z. M. Kurenbaeva, A. I. Tursina, E. V. Murashova, S. N. Nesterenko, A. V. Gribanov, Y. D. Seropegin, H. Noël, *J. Alloys Compd.* **2007**, *442*, 86.

[2] E. V. Murashova, Z. M. Kurenbaeva, A. I. Tursina, H. Noël, P. Rogl, A. V. Grytsiv, A. V. Gribanov, G. Giester, Y. D. Seropegin, *J. Alloys Compd.* **2007**, *442*, 89.

[3] A. I. Tursina, Z. M. Kurenbaeva, A. V. Gribanov, H. Noël, T. Roisnel, Y. D. Seropegin, *J. Alloys Compd.* **2007**, *442*, 100.

[4] E. V. Murashova, A. I. Tursina, Z. M. Kurenbaeva, A. V. Gribanov, Y. D. Seropegin, *J. Alloys Compd.* **2008**, *454*, 206.

[5] J. F. Riecken, W. Hermes, B. Chevalier, R.-D. Hoffmann, F. M. Schappacher, R. Pöttgen, *Z. Anorg. Allg. Chem.* **2007**, *633*, 1094.

[6] S. F. Matar, J. F. Riecken, B. Chevalier, R. Pöttgen, A. F. Al Alam, V. Eyert, *Phys. Rev. B* **2007**, *76*, 174434.

[7] J. Mydosh, A. M. Strydom, M. Baenitz, B. Chevalier, W. Hermes, B. Chevalier, *Phys. Rev. B* **2011**, *83*, 054411.

[8] R. Mishra, W. Hermes, U. C. Rodewald, R.-D. Hoffmann, R. Pöttgen, *Z. Anorg. Allg. Chem.* **2008**, *634*, 470.

[9] V. Eyert, E.-W. Scheidt, W. Scherer, W. Hermes, R. Pöttgen, *Phys. Rev. B* **2008**, *78*, 214420.

[10] C. Schank, F. Jährling, L. Luo, A. Grauel, C. Wassilew, R. Borth, G. Olesch, C. D. Bredl, C. Geibel, F. Steglich, *J. Alloys Compd.* **1994**, *207/208*, 329.

[11] A. V. Gribanov, A. I. Tursina, A. V. Grytsiv, E. V. Murashova, N. G. Bukhan'ko, P. Rogl, Y. D. Seropegin, G. Giester, *J. Alloys Compd.* **2008**, *454*, 164.

[12] W. Hermes, S. F. Matar, R. Pöttgen, *Z. Naturforsch.* **2009**, *64b*, 901.

[13] S. Linsinger, M. Eul, U. C. Rodewald, R. Pöttgen, *Z. Naturforsch.* **2010**, *65b*, 1185.

[14] S. Linsinger, M. Eul, W. Hermes, R.-D. Hoffmann, R. Pöttgen, *Z. Naturforsch.* **2009**, *64b*, 1345.

[15] F. Tappe, W. Hermes, M. Eul, R. Pöttgen, *Intermetallics* **2009**, *17*, 1035.

[16] S. Tuncel, B. Chevalier, S. F. Matar, R. Pöttgen, *Z. Anorg. Allg. Chem.* **2007**, *633*, 2019.

[17] J. F. Riecken, A. F. Al Alam, B. Chevalier, S. F. Matar, R. Pöttgen, *Z. Naturforsch.* **2008**, *63b*, 1062.

[18] S. Linsinger, R. -D. Hoffmann, R. Pöttgen, unpublished results.

[19] K. Schubert, K. Frank, R. Gohle, A. Maldonado, H. G. Meissner, A. Raman, W. Rossteutscher, *Naturwissenschaften* **1963**, *50*, 41.

[20] R. Pöttgen, T. Gulden, A. Simon, *GIT Labor-Fachzeitschrift* **1999**, *43*, 133.

[21] K. Yvon, W. Jeitschko, E. Parthé, *J. Appl. Crystallogr.* **1977**, *10*, 73.

[22] G. M. Sheldrick, SHELXS-97, Program for the Solution of Crystal Structures, University of Göttingen, Göttingen (Germany) **1997**. See also: G. M. Sheldrick, *Acta Crystallogr.* **1990**, *A46*, 467.

[23] G. M. Sheldrick, SHELXL-97, Program for the Refinement of Crystal Structures, University of Göttingen, Göttingen (Germany) **1997**. See also: G. M. Sheldrick, *Acta Crystallogr.* **2008**, *A64*, 112.

[24] P. Villars, K. Cenzual, *Pearson's Crystal Data: Crystal Structure Database for Inorganic Compounds*, (release 2009/10), ASM International®, Materials Park, Ohio **2009/2010**.

[25] F. S. Kreidenko, V. Ya. Markiv, E. M. Sokolovskaya, *Mosc. Univ. Chem. Bull.* **1974**, *29*, 83.

[26] S. V. Popova, V. G. Putro, *Inorg. Mater.* **1979**, *15*, 947.

[27] V. Y. Markiv, N. N. Belyavina, *Russ. Metallurgy* **1986**, *6*, 204.

[28] V. Y. Markiv, A. I. Skripta, *Russ. Metallurgy* **1986**, *6*, 196.

[29] N. O. Koblyuk, L. G. Akselrud, R. V. Skolozdra, *Polish J. Chem.* **1999**, *73*, 1465.

[30] H. Kleinke, *J. Solid State Chem.* **2001**, *159*, 134.

[31] L. M. Gelato, E. Parthé, *J. Appl. Crystallogr.* **1987**, *20*, 139.

[32] E. Parthé, L. M. Gelato, *Acta Crystallogr.* **1984**, *A40*, 169.

[33] J. Emsley, *The Elements*, Oxford University Press, Oxford **1999**.

[34] A. Palenzona, *J. Less-Common Met.* **1979**, *66*, P27.

[35] J. Donohue, *The Structures of the Elements*, Wiley, New York **1974**.

[36] U. C. Rodewald, B. Chevalier, R. Pöttgen, *J. Solid State Chem.* **2007**, *180*, 1720.

[37] P. Solokha, S. De Negri, V. Pavlyuk, A. Saccone, B. Marciniak, *J. Solid State Chem.* **2007**, *180*, 3066.